Behavioral/Systems/Cognitive

Na^+–Ca^{2+} Exchanger (NCX3) Knock-Out Mice Display an Impairment in Hippocampal Long-Term Potentiation and Spatial Learning and Memory

Pasquale Molinaro,[1] Davide Viggiano,[1] Robert Nisticò,[2,3] Rossana Sirabella,[4] Agnese Secondo,[1,6] Francesca Boscia,[4] Anna Pannaccione,[1,6] Antonella Scorziello,[1,6] Bisan Mehdawy,[2] Sophie Sokolow,[5] André Herchuelz,[5] Gianfranco F. Di Renzo,[1,6] and Lucio Annunziato[1,4,6]

[1]Division of Pharmacology, Department of Neuroscience, School of Medicine, "Federico II" University of Naples, 80131 Naples, Italy, [2]Centro Europeo per la Ricerca sul Cervello/Fondazione Santa Lucia, 64-00143 Rome, Italy, [3]Department of Pharmacobiology, University of Calabria, 87036 Arcavacata di Rende, Italy, [4]Fondazione Istituto di Ricovero e Cura a Carattere Scientifico SDN, 80143 Naples, Italy, [5]Laboratory of Pharmacology and Therapeutics, Université Libre de Bruxelles, Brussels, 6041 Gosselies, Belgium, and [6]National Institute of Neuroscience, 10125 Turin, Italy

Long-term potentiation (LTP) depends on the coordinated regulation of an ensemble of proteins related to Ca^{2+} homeostasis, including Ca^{2+} transporters. One of the major players in the regulation of intracellular Ca^{2+} ($[Ca^{2+}]_i$) homeostasis in neurons is the sodium/calcium exchanger (NCX), which represents the principal mechanism of Ca^{2+} clearance in the synaptic sites of hippocampal neurons. Because NCX3, one of the three brain isoforms of the NCX family, is highly expressed in the hippocampal subfields involved in LTP, we hypothesized that it might represent a potential candidate for LTP modulation. To test this hypothesis, we first examined the effect of *ncx3* gene ablation on NCX currents (I_{NCX}) and Ca^{2+} homeostasis in hippocampal neurons. *ncx3*$^{-/-}$ neurons displayed a reduced I_{NCX}, a higher basal level of $[Ca^{2+}]_i$, and a significantly delayed clearance of $[Ca^{2+}]_i$ following depolarization. Furthermore, measurement of field EPSPs, recorded from the CA1 area, revealed that *ncx3*$^{-/-}$ mice had an impaired basal synaptic transmission. Moreover, hippocampal slices from *ncx3*$^{-/-}$ mice exhibited a worsening in LTP compared with congenic *ncx3*$^{+/+}$. Consistently, immunohistochemical and immunoblot analysis indicated that in the hippocampus of *ncx3*$^{-/-}$ mice both Ca^{2+}/calmodulin-dependent protein kinase IIα (CaMKIIα) expression and the phosphoCaMKIIα/CaMKIIα ratio were significantly reduced compared with *ncx3*$^{+/+}$. Interestingly, *ncx3*$^{-/-}$ mice displayed a reduced spatial learning and memory performance, as revealed by the novel object recognition, Barnes maze, and context-dependent fear conditioning assays. Collectively, our findings demonstrate that the deletion of the *ncx3* gene in mice has detrimental consequences on basal synaptic transmission, LTP regulation, spatial learning, and memory performance.

Introduction

Excitatory synapses in the brain show several forms of synaptic plasticity, including long-term potentiation (LTP) and long-term depression (LTD), that depend on the regulation of many signaling pathways. LTP mainly relies on the coordinated regulation of an ensemble of proteins related to Ca^{2+} homeostasis, including Ca^{2+}/calmodulin-dependent protein kinase IIα (CaMKIIα), adenylyl cyclase 1 and 8, calcineurin, and Ca^{2+} channels and transporters. The CA1 region of the hippocampus is the prototypical site of mammalian LTP studies. In particular, LTP at the hippocampal Schaffer collateral-CA1 synapse level is initiated by increases in intracellular Ca^{2+} ($[Ca^{2+}]_i$) generated by *N*-methyl-D-aspartate receptor and voltage-sensitive Ca^{2+} channel activation. One of the major players in the regulation of $[Ca^{2+}]_i$ homeostasis is the sodium/calcium exchanger (NCX), which represents the principal mechanism of Ca^{2+} clearance at the synaptic site of hippocampal neurons (Reuter and Porzig, 1995). NCX comprises three isoforms, NCX1, NCX2, and NCX3, highly expressed in the brain (Quednau et al., 1997; Papa et al., 2003) and involved in several pathophysiological conditions (Pignataro et al., 2004; Boscia et al., 2006; Secondo et al., 2007). In particular, high levels of mRNA and protein encoded by the three NCX genes are present in the granule cell layer of the dentate gyrus as well as in the pyramidal cells of the CA1 and CA3 subfields (Papa et al., 2003; Annunziato et al., 2004). These regions are involved in LTP at hippocampal Schaffer collateral synapses (Skeberdis et

Received Dec. 3, 2010; revised Feb. 10, 2011; accepted Feb. 27, 2011.

Author contributions: P.M., D.V., and L.A. designed research; D.V., R.N., A.Se., F.B., A.P., A.Sc., B.M., and R.S. performed research; S.S. and A.H. contributed unpublished reagents/analytic tools; P.M., D.V., R.N., A.Se., F.B., A.P., B.M., and R.S. analyzed data; P.M., D.V., A.Se., F.B., G.F.D.R., and L.A. wrote the paper.

This work was supported by COFIN 2006; by "Ministero Affari Esteri, Direzione Generale per la Promozione e la Cooperazione Culturale Fondi Italia-Cina Legge 401/1990 2007, 2008"; Ministero della Salute, Ricerca Sanitaria RF-FSL352059 Ricerca Finalizzata 2006; Ministero della Salute, Ricerca Oncologica 2006; Ministero della Salute, Progetto Strategico 2007; and Ministero della Salute, Progetto Ordinario 2007 (all to L.A.). We thank Dr. Margherita Fusco for her help in behavioral tests, Dr. Paola Merolla for editorial revision, and Vincenzo Grillo and Carmine Capitale for technical support.

*P.M. and D.V. equally contributed to this work.

Correspondence should be addressed to Dr. Lucio Annunziato, Division of Pharmacology, Department of Neuroscience, School of Medicine, "Federico II" University of Naples, Via Pansini 5, 80131 Naples, Italy. E-mail: lannunzi@unina.it.

S. Sokolow's present address: University of California, Los Angeles School of Nursing, Los Angeles, CA 90095.

B. Mehdawy's present address: IRCCS Neurological Institute "C. Mondino", 27100 Pavia, Italy.

DOI:10.1523/JNEUROSCI.6296-10.2011

 0270-6474/11/317312-10$15.00/0

al., 2006). Interestingly, in the oriens and radiatum layers of the CA1 area, immunostaining for NCX3 is more intense than that for NCX1 and NCX2. In the CA3 area, NCX1 and NCX3 immunoreactivity of mossy fibers projecting from the granule cells located in the dentate gyrus is much more intense than that of NCX2. Thus, given the particular distribution of NCX3 in the hippocampus, we evaluated whether: (1) a change in $[Ca^{2+}]_i$ homeostasis occurs in *ncx3*$^{-/-}$ hippocampal neurons; (2) an alteration of LTP might be observed in *ncx3*$^{-/-}$ hippocampal Schaffer collateral-CA1 synapses; and (3) *ncx3*$^{-/-}$ mice exhibit a consequent alteration of spatial learning and memory performance.

To these aims, we measured $[Ca^{2+}]_i$ in primary cultures of hippocampal neurons by single-cell microfluorimetry, and examined basal transmission and synaptic plasticity in hippocampal slices from *ncx3*$^{-/-}$ mice. In particular, the field EPSPs (fEPSPs) were recorded from the CA1 area of hippocampus in response to stimulation of Schaffer collateral fibers at increasing stimulus intensity. Then, we investigated the presynaptic role of NCX3 in neurotransmission through the paired-pulse facilitation (PPF), a transient enhancement of neurotransmitter release induced by two closely spaced stimuli. Furthermore, we compared the expression of CaMKIIα, a calcium-related protein mainly involved in CA1-dependent LTP, and the phosphoCaMKIIα/CaMKIIα ratio in the hippocampus of *ncx3*$^{-/-}$ mice to that of congenic *ncx3*$^{+/+}$ mice.

Finally, the performance of *ncx3*$^{-/-}$ mice was tested by several hippocampus-dependent learning and memory tasks, such as novel object recognition, Barnes' maze, and trace fear conditioning tests.

The results obtained in the present study indicate that NCX3 plays an essential role in LTP, and spatial learning and memory processes.

Materials and Methods

Experimental groups

NCX3 knock-out mice were generated by our research group as previously described (Sokolow et al., 2004). Genetic background of *ncx3*$^{-/-}$ and *ncx3*$^{+/+}$ mice were obtained by backcrossing *ncx3*$^{-/-}$ mice (Sv129) against C57BL/6 Charles River mice for 6 generations. *ncx3*$^{+/+}$ and *ncx3*$^{-/-}$ mice, aged 6–8 weeks and weighing 27–30 g, were housed under diurnal lighting conditions. Experiments were performed on male mice according to the international guidelines for animal research and approved by the Animal Care Committee of "Federico II" University of Naples, Italy.

Primary hippocampal neurons cultures

Hippocampal neurons were prepared from brains of 14-d-old mouse embryos, plated on coverslips, and cultured in MEM/F12 (Invitrogen) containing glucose, 5% of deactivated fetal bovine serum, 5% horse serum (Invitrogen), glutamine (2 mM), penicillin (50 U/ml), and streptomycin (50 μg/ml). Cytosine-β-D-arabinofuranoside (10 μM) was added within 48 h of plating to prevent the growth of non-neuronal cells. Neurons were cultured at 37°C in a humidified 5% CO_2 atmosphere and used after 7–10 d *in vitro* (DIV) (Carlucci et al., 2008).

$[Ca^{2+}]_i$ measurement

$[Ca^{2+}]_i$ was measured by single-cell computer-assisted video imaging in hippocampal neurons loaded with 10 μM Fura-2 acetoxymethyl ester (Fura-2 AM) (EMD Biosciences; 30 min, room temperature) (Secondo et al., 2007). At the end of the loading period, the coverslips were placed into a perfusion chamber (Medical Systems) mounted onto a Zeiss Axiovert 200 microscope connected with a digital imaging system composed of MicroMax 512BFT cooled CCD camera (Princeton Instruments), Lambda 10-2 filter wheeler (Sutter Instruments), and MetaMorph/MetaFluor Imaging System software (Universal Imaging). Fura-2 AM fluorescence intensity was measured every 3 s and $[Ca^{2+}]_i$ was calculated by a preloaded calibration curve obtained in preliminary experiments (Grynkiewicz et al., 1985).

Electrophysiology

Whole-cell patch-clamp analysis. NCX currents (I_{NCX}) were recorded from *ncx3*$^{+/+}$ and *ncx3*$^{-/-}$ primary hippocampal neurons at 20−22°C by patch-clamp technique in whole-cell configuration using a commercially available amplifier (Molecular Devices) as previously described (Molinaro et al., 2008). I_{NCX} was recorded starting from a holding potential of −60 mV up to a short-step depolarization at +60 mV (60 ms). Then, a descending voltage ramp from +60 mV to −120 mV was applied. The current recorded in the descending portion of the ramp (from +60 mV to −120 mV) was used to plot the current–voltage (*I–V*) relation curve. The magnitude of I_{NCX} was measured at the end of +60 mV (reverse mode) and at the end of −120 mV (forward mode), respectively. The Ni^{2+}-insensitive component was subtracted from total currents to isolate I_{NCX}. In addition, the potassium, sodium and calcium currents were abolished by means of TEA (20 mM), TTX (50 nM) and nimodipine (10 μM).

Extracellular recording in hippocampal CA1. Preparation of hippocampal slices was performed in accordance with the European Communities Council Directive (86/609/EEC). Vibratome-cut parasagittal slices (400 μm) were prepared, incubated for 1 h and then transferred to a recording chamber submerged in a continuously flowing artificial CSF (30°C, 2–3 ml/min) gassed with 95% O_2 and 5% CO_2. The composition of the control solution was (in mM): 126 NaCl, 2.5 KCl, 1.2 $MgCl_2$, 1.2 NaH_2PO_4, 2.4 $CaCl_2$, 11 glucose, 25 $NaHCO_3$. fEPSPs were recorded in the stratum radiatum of the CA1 using glass microelectrodes (1–5 MΩ) filled with artificial CSF. Synaptic responses were evoked by stimulation of the Schaffer collateral/commissural pathway with a concentric bipolar stimulating electrode. Stimulus–response curves were constructed by using stimulus intensities from 0 to 50 mV at 5 mV increments. Responses were subsequently set to a level that yielded a slope value 30% of the maximal response. Baseline responses were obtained every 30 s. PPF was assessed using a succession of paired pulses separated by intervals of 20, 50, 100, 200, and 500 ms. An additional 30 min baseline period was obtained before attempting to induce LTP. LTP was induced by a high-frequency stimulation (HFS) protocol (1 train, 100 Hz, 1 s) and the effect of conditioning train was expressed as the mean (±SEM) percentage of baseline EPSP slopes measured at 60 min after stimulation protocol. Data were expressed as mean ± SEM and assessed for significance using the Student's *t* test.

Protein expression analysis

Whole-cell protein extracts from adult hippocampus and from embryonic hippocampal and cortical neurons of *ncx3*$^{+/+}$ and *ncx3*$^{-/-}$ mice were obtained and processed as previously described (Molinaro et al., 2008). Nitrocellulose-membranes were incubated with anti-NCX3 antibody (rabbit polyclonal, 1:2000, kindly provided by K. D. Philipson and D. A. Nicoll, University of California, Los Angeles, Los Angeles, CA) or anti-Phospho-CaM Kinase IIα (mouse monoclonal, 1:1000, Thermo Scientific, Rockford, IL), or anti-CaM Kinase IIα (rabbit polyclonal, 1:500, Thermo Scientific, Rockford, IL) or anti-β-actin (mouse monoclonal, 1:1000, Sigma-Aldrich).

These nitrocellulose-membranes were first washed with 0.1% Tween 20, and then incubated with the corresponding secondary antibodies for 1 h (GE Healthcare Bio-Sciences). Immunoreactive bands were detected with electrochemiluminescence (GE Healthcare Bio-Sciences). The optical density of the bands (normalized with β-actin or CaMKIIα) was determined by Chemi-Doc Imaging System (Bio-Rad).

Immunohistochemistry and image analysis

For the morphological studies, mice were transcardially perfused with 4% paraformaldehyde in 0.1 M phosphate buffer, pH 7.4, and fixed at 4°C. After cryoprotection and freezing, 20-μm-thick cryosections at the level of the dorsal hippocampal formation were mounted on SuperFrost Plus slides and stored at −80°C.

Immunohistochemistry for CaMKIIα protein was performed as follows: slides were rinsed in PBS and then incubated with a mouse mono-

clonal anti-CaMKIIα (1:100, Sigma, clone 6G9) in PBS overnight in agitation at +4°C. To allow optimal homogeneous staining among slices, the HybriWell system was used (Sigma-Aldrich). After three rinses in PBS, sections were then incubated with anti-mouse biotinylated antibody (1:100, Vector Laboratories) for 1 h at room temperature in agitation, and the ABC MOM system (Vector Laboratories) was used to visualize the reaction product (prepared according the supplier's instructions). The reaction was visualized using DAB as chromogen. All staining and morphological analyses were blindly conducted. Slides were analyzed with a Zeiss Axioskop 20, equipped with a CCD high-resolution camera (Hamamatsu Photonics, C5405) and a motorized XYZ stage (ProScan II, Prior Scientific). To minimize potential aspecific signals in fluorescence emission and densitometric analysis, all brain sections from all animals were stained in only one session, at the same time with the same solutions and the same incubation times. Moreover, sections were acquired in the same session, randomizing the sequence of the acquisitions across brains. In addition, the laser of confocal microscope, for fluorescent imaging, and the lamp of the microscope, for immunohistochemistry, were always turned on at least 20 min before the use to achieve light stability. Moreover, to test the stability of the light, random sections were also acquired at the end of the acquisition session. The entire hippocampus was acquired using tiled fields from 10× objective (MCID Elite; Imaging Research Inc.). Images were quantitatively analyzed as already described (Capowski, 1989). At least 10 slices per brain were imaged for each staining technique.

CaMKIIα expression levels were quantified in the pyramidal layer of the CA1 and CA3 regions and in the granules of the dentate gyrus (DG), as relative optical density units (ROD = log [256/gray level]). ROD units, after background subtraction, are correlated to the antigen concentration (Burke et al., 1990). Images were then represented using a pseudocolor scale.

Confocal imaging for NeuN and synaptophysin

Frozen hippocampal cryosections were incubated overnight at 4°C with a mixture of mouse anti-NeuN (1:100, Millipore), or rabbit anti-NCX3 (1:5000, kindly provided by Dr. D. A. Nicoll and K. D. Philipson) and mouse anti-PSD95 (1:500, Millipore). Separate sections were incubated with mouse anti-synaptophysin (1:1000, Millipore) a widely used marker for the quantification of synapse number. Primary antibodies were diluted in 10% normal serum in PBS and incubations were performed using the HybriWell system to ensure homogeneous staining (Sigma-Aldrich).

Slices were then washed in PBS and incubated at room temperature for 1 h, in a mixture containing two fluorescent secondary antibodies: anti-mouse IgG conjugated to CY2 (cyanine 2) (Jackson Laboratories) for anti-NeuN or for anti-PSD95 antibodies, anti-rabbit IgG conjugated to CY3 (Jackson Laboratories) for anti-NCX3 and for synaptophysin (Millipore), all of which were diluted 1:100 in PBS containing 10% albumin bovine serum. Subsequently, sections were first washed in PBS, then allowed to air dry and, finally, mounted in SlowFade antifade solution (Invitrogen) before coverslipping.

Slides were analyzed using the Zeiss LSM 512 argon/krypton laser scanning confocal microscope. The laser scanning confocal microscope was set to multitrack acquisition state to avoid fluorescence bleed from one fluorochrome to the other. The excitation/emission settings were as follows: 488 nm line of excitation of the argon/krypton laser and 505–550 nm emission filter for CY2, 543 nm line of excitation and emission, detected at 560–615 nm, for CY3-labeled structures. Hippocampal regions and cell cultures were confocally captured using ×10, ×40, and ×100 objectives. Each optical section was filtered using a 4-times averaging filter to improve signal/noise ratio.

The color scheme was red for CY3-labeled structures, and green for CY2-labeled structures. After image acquisition, the signal intensity was quantified using NIH ImageJ software. To this aim, the average gray level corresponding to the soma of either granule cells was obtained subtracting the background signal.

For PSD-95 (postsynaptic density 95 protein) and NCX3 colocalization, immunofluorescent images were first thresholded to identify a positive signal; subsequently the pixels expressing both NCX3 and PSD-95 were identified using an AND operational command in NIH ImageJ. Finally the number of pixels positive for both NCX3 and PSD-95 were measured and expressed as percentage of total number of pixels positive for NCX3. Results form several images were then analyzed.

For the quantification of synapse number, synaptophysin immunosignal was used as a marker. To quantify the number of synaptophysin-positive puncta, images were first thresholded and subsequently the number of particles automatically counted using a specific NIH ImageJ function. Moreover, the total fluorescence intensity of synaptophysin-positive terminals was also measured in the same CA1 area of both *ncx3*$^{+/+}$ and *ncx3*$^{-/-}$ mice using NIH ImageJ.

Behavioral studies

At the age of 2 months mice were behaviorally tested. Experiments were performed during the light phase between 10:00 A.M. and 5:00 P.M. Exploratory behavior was acquired with a high definition digital camera and on-line videotracking was computed using a custom software written in Matlab environment.

Open-field exploration

The open field apparatus consisting of a transparent Plexiglas square arena (50 × 50 cm, 40 cm high) was placed in a homogenously lit experimental room with several large-scale environmental visual cues. Briefly, mice were placed in the arena and were allowed to explore it for 5 min. Total traveled distance was measured using an automated tracking device. Moreover, the time spent by animals in three concentric areas was automatically measured as an index of anxious behavior (Kassed and Herkenham, 2004; Kazlauckas et al., 2005). Since the probability to explore an area is proportional to the size of the area, the time spent in each area was also divided by the percentage size of the total area to obtain unbiased estimates.

At the end of the test, the number of fecal boluses was counted to evaluate anxious behavior. The same apparatus was also used for the object recognition task.

Delay-dependent one-trial object recognition task

Object features. Two different objects that differed in terms of height, color, shape, and surface texture were used. Both of them had sufficient weight to ensure that the mice could not displace them, had no ethological significance for the mice, and had never been paired with a reinforcer. Indeed, pilot studies have ensured that mice of the C57BL/6J genetic background strain cannot discriminate between objects and have no preference for one object over another (Ennaceur and Delacour, 1988; Dere et al., 2007).

Procedure. Mice were subjected to two types of trials: a sample trial and a test trial. During the sample trial, which took place 1 d after exposure to the open field so as to allow the animals to habituate to the test apparatus, all mice were presented with the first pair of identical objects. Briefly, the animal was placed on one side of the open field, whereas, on the opposite side, two copies of the same objects were placed 10 cm from the two corners. After 5 min, the animal was removed from the open field and were returned to their home cage (Ennaceur and Delacour, 1988; Dere et al., 2007).

During the trial phase, instead, *ncx3*$^{+/+}$ and *ncx3*$^{-/-}$ mice were tested for item recognition (5 min) 2 or 24 h after sample trial phase. The animal was again released into the open field, now containing two objects: the familiar one used during the sample trial and the novel object, which was randomly positioned (Ennaceur and Delacour, 1988; Dere et al., 2007).

The time spent by each mouse in exploring the two objects was then recorded. Exploration of an object was assumed when the mouse approached an object, when touched it with either its vibrissae, snout, or forepaws. The percentage of time spent exploring the novel object, compared with the total time spent exploring both objects, was recorded and considered as a measure of object recognition: recognition index = $t_{novel}/(t_{novel} + t_{familiar}) \times 100$. Recognition index values >50 suggest a preference for the novel object, values close to 50 suggest no recognition, and values well below 50 suggest a preference for the familiar object (Ennaceur and Delacour, 1988; Kassed and Herkenham, 2004; Kazlauckas et al., 2005; Dere et al., 2007).

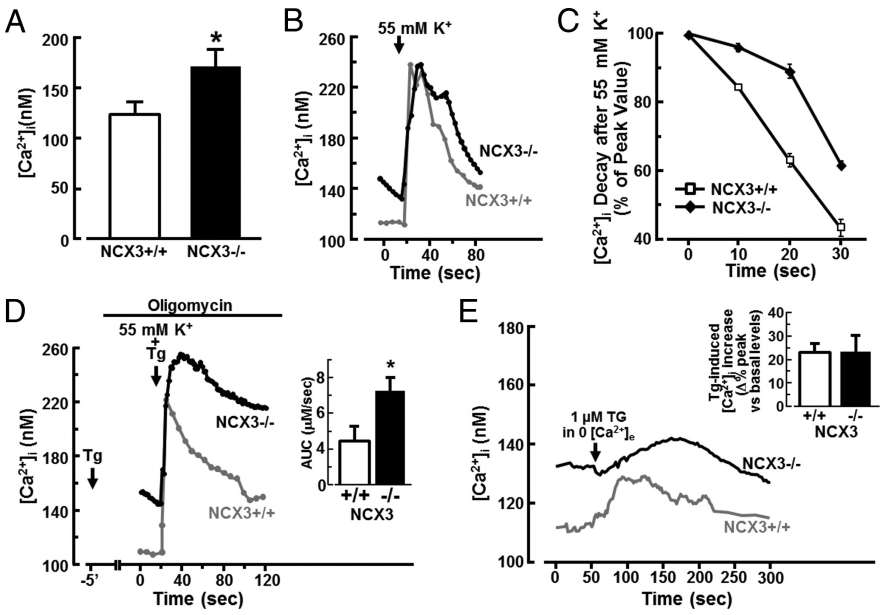

Figure 1. Effect of NCX3 genetic ablation on $[Ca^{2+}]_i$ in hippocampal neurons. ***A***, Quantification of $[Ca^{2+}]_i$ basal levels in *ncx3* $^{+/+}$ and *ncx3* $^{-/-}$ primary hippocampal neurons. The data are the mean ± SE of three independent experiments. ***B***, Representative superimposed single-cell traces for the effect of 55 mM K^+ on $[Ca^{2+}]_i$ in 10 DIV hippocampal neurons from *ncx3* $^{+/+}$ and *ncx3* $^{-/-}$ mice. For each experiment, 40–65 individual cells were monitored. ***C***, $[Ca^{2+}]_i$ decay kinetics after 55 mM K^+ perfusion. The decay constant in *ncx3* $^{+/+}$ and *ncx3* $^{-/-}$ was obtained by fitting a single exponential to the data expressed as percentage of the peak of 55 mM K^+-induced $[Ca^{2+}]_i$ changes. For each experiment, 40–50 individual cells were monitored. The data are the mean ± SE of three independent experiments. ***D***, Superimposed single-cell traces representing the effect of 55 mM K^+ on $[Ca^{2+}]_i$ in 10 DIV hippocampal neurons from *ncx3* $^{+/+}$ and *ncx3* $^{-/-}$ mice, after preincubation with 1 μM oligomycin for 20 min and 1 μM thapsigargin (Tg) for 5 min. For each experiment, 40–65 individual cells were monitored. The inset of ***D*** depicts the quantification of the area under the curve (AUC) of $[Ca^{2+}]_i$ increase elicited by 55 mM K^+ in *ncx3* $^{+/+}$ and *ncx3* $^{-/-}$ hippocampal neurons. The data are the mean ± SE of three independent experiments. *$p < 0.05$ versus *ncx3* $^{+/+}$. ***E***, Superimposed single-cell traces representing the effect of Tg (1 μM) + 0 Ca^{2+} in *ncx3* $^{+/+}$ and *ncx3* $^{-/-}$ hippocampal neurons. The inset of the panel represents the quantification of the amount of Ca^{2+} released from ER in *ncx3* $^{+/+}$ and *ncx3* $^{-/-}$ hippocampal neurons. The data are the mean ± SE of three independent experiments. For each experiment, 20–35 individual cells were monitored.

Trace fear conditioning

The trace fear conditioning procedure is a modified form of tone (delay) fear conditioning because it demands a "trace interval" between the unconditioned stimulus (US) and conditioned stimulus (CS). Unlike delay tone conditioning, the acquisition of trace fear conditioning is sensitive to hippocampal lesions (McEchron et al., 1998; Desmedt et al., 2003; Bangasser et al., 2006) and to genetic modifications of the hippocampus (Huerta et al., 2000; D'Adamo et al., 2002). A fear-conditioning shock chamber (35 × 23 cm, 19 cm height) containing a stainless steel rod floor (2.5 mm diameter, spaced 1 cm apart, Ugo Basile Inc.) and a high definition digital camera to monitor animal movements were used. The apparatus for on-line tracking and stimulus/shock delivery was controlled using a custom software developed in Matlab environment. Briefly, for the conditioning (Lu et al., 1997; Jeon et al., 2003), mice were first placed in the fear-conditioning apparatus chamber for 5 min (habituation phase), and, then, a 15 s acoustic CS (1000 Hz, 80 dB) was delivered. The tone intensity and frequency, previously tested in C57BL/6J mice, did not evoke freezing before conditioning although short orienting reactions showed their ability to perceive the sound. After 15 s from the end of the acoustic stimulus, a 0.5 mA shock (0.8 s duration) of unconditioned stimulus was applied to the floor grid. This protocol was repeated for 5 times every 30 s (intertrial interval).

Context test of trace fear conditioning was measured 2 h after the conditioning procedure. Animals were tested for their context freezing response and afterward for their response to the tone in a different context. Context freezing response was measured placing the animals for 1 min in the same apparatus used for conditioning in absence of electrical or acoustical stimuli. Behavior was recorded with a digital camera and off-line analyzed for the freezing behavior, defined as complete absence of somatic movements except for respiratory movements.

To assess the tone test in trace fear conditioning, the animals were placed in a different context (novel chamber, odor, floor, and visual cues) 15 min after the context test, and their behavior was monitored for 3 min. All experimental groups were observed for 30 s before the tone (pre-CS) in the new context to verify baseline activity. Data showed no differences in baseline activity expressed as percentage of freezing time (*ncx3* $^{+/+}$, 6.61 ± 3.5%; *ncx3* $^{-/-}$, 5.06 ± 3.2%; $p > 0.05$). After 30 s of observation in the new context, animals were exposed to the tone for 1 min. Fear response was quantified by measuring the duration of freezing behavior by using a custom software. Freezing behavior was defined as a total lack of movement, apart from respiration, with a crouching position. In addition to freezing responses, the animals' locomotor activity was recorded by a video tracking system.

Barnes circular maze task

Apparatus. The behavioral apparatus used in this experiment consisted of a white circular platform (1.22 m diameter) elevated 40 cm above the floor, with 36 equally spaced holes (each 5 cm diameter) around the periphery (5 cm from the perimeter). Only one hole led to a dark escape box (5 cm × 5 cm × 11 cm) that was fixed in relation to the distal environmental cues and contained some dust-free sawdust bedding which was changed between trials. The platform surface was randomly rotated from trial to trial to prevent the use of local olfactory, visual, or tactile cues and was brightly illuminated from above. The illumination served as motivation to escape in the dark box (Bach et al., 1995; Seeger et al., 2004).

Procedure. Mice were gently picked up from the tail and placed in the middle of the platform. The direction faced by the animals at the start position was random and changed from trial to trial. After 5 min, if the mice did not find the goal they were gently directed toward the correct hole, and allowed to descend into the escape box where they were left for 1 min (Bach et al., 1995; Seeger et al., 2004).

On the following 5 d, test trials (one trial per day) were performed under identical conditions. Each trial ended when the mouse entered the goal tunnel or after a maximum time of 5 min. The amount of time it took the mice to enter the escape hole (escape latency) was recorded (Bach et al., 1995; Seeger et al., 2004).

Statistical analysis

Values are expressed as means ± SE. Statistical analysis was performed with Student's *t* test, Kruskal–Wallis test or two-way ANOVA followed by Dunnett's test. Statistical significance was accepted at the 95% confidence level ($p < 0.05$).

Results

NCX3 genetic ablation increases basal $[Ca^{2+}]_i$ and delays $[Ca^{2+}]_i$ clearance in hippocampal neurons

$[Ca^{2+}]_i$ levels during resting conditions were significantly higher in primary *ncx3* $^{-/-}$ hippocampal neurons than in congenic *ncx3* $^{+/+}$ (Fig. 1*A*). Moreover, the decline in $[Ca^{2+}]_i$ following 55 mM K^+-induced peak was significantly slower in *ncx3* $^{-/-}$ hippocampal neurons than in *ncx3* $^{+/+}$, as shown by the higher values of the $[Ca^{2+}]_i$ decay constant in *ncx3* $^{-/-}$ neurons ($\tau = 31 \pm 5$ s), compared with that of congenic *ncx3* $^{+/+}$ neurons ($\tau = 17 \pm$

0.7 s) (Fig. 1*B*,*C*). However, the lack of NCX3 did not affect peak values of $[Ca^{2+}]_i$ after stimulation with 55 mM K^+ (Fig. 1*B*). Interestingly, the slower declining rate of $[Ca^{2+}]_i$ after 55 mM K^+-induced depolarization in NCX3 knock-out was much more evident when neurons were exposed to both oligomycin (1 μM/20 min)—an ATP depletor—and thapsigargin (1 μM), a smooth endoplasmic reticulum Ca^{2+}-ATPase (SERCA) inhibitor (Fig. 1*D*). Indeed, the area under the curve of the $[Ca^{2+}]_i$ response to 55 mM K^+ exposure was significantly higher for *ncx3* $^{-/-}$ hippocampal neurons than for *ncx3* $^{+/+}$ (Fig. 1*D*, inset).

In contrast, the release of Ca^{2+} from the endoplasmic reticulum (ER), induced by the SERCA inhibitor, thapsigargin, was not affected by the lack of NCX3 in hippocampal neurons (Fig. 1*E*), thus demonstrating that, in resting conditions, NCX3 does not interfere with Ca^{2+} storage in the ER.

NCX3 knocking-down reduces I_{NCX} in primary hippocampal neurons

NCX activity was assessed in primary hippocampal neurons from *ncx3* $^{+/+}$ and *ncx3* $^{-/-}$ mice by patch-clamp technique in whole-cell configuration using the ramp protocol (see Materials and Methods). I_{NCX}, recorded in both forward and reverse modes of operation by the whole-cell patch-clamp technique, was significantly lower in primary hippocampal neurons obtained from *ncx3* $^{-/-}$ mice than in those obtained from congenic *ncx3* $^{+/+}$ (Fig. 2*A*,*B*). Western blot analysis showed that NCX3 protein expression was undetectable in embryonic neurons obtained from *ncx3* $^{-/-}$ mice (Fig. 2*C*).

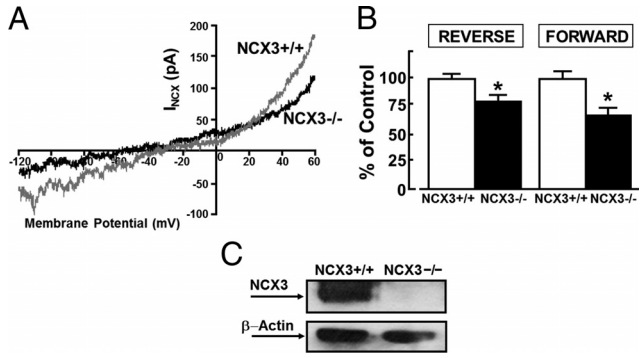

Figure 2. Effect of NCX3 knock-out on I_{NCX} recorded in the reverse and forward modes of operation in hippocampal neurons. ***A***, I_{NCX} superimposed traces recorded from *ncx3* $^{+/+}$ and *ncx3* $^{-/-}$ hippocampal neurons. ***B***, I_{NCX} quantification, expressed as percentage of wild-type and recorded in the forward and reverse modes of operation in *ncx3* $^{+/+}$ and *ncx3* $^{-/-}$ hippocampal neurons. Each bar represents the mean (±SEM) of the values obtained from almost 20 cells in three independent experimental sessions. *$p < 0.05$ versus congenic *ncx3* $^{+/+}$. ***C***, Western blot analysis of primary neurons from *ncx3* $^{-/-}$ and *ncx3* $^{+/+}$ mice.

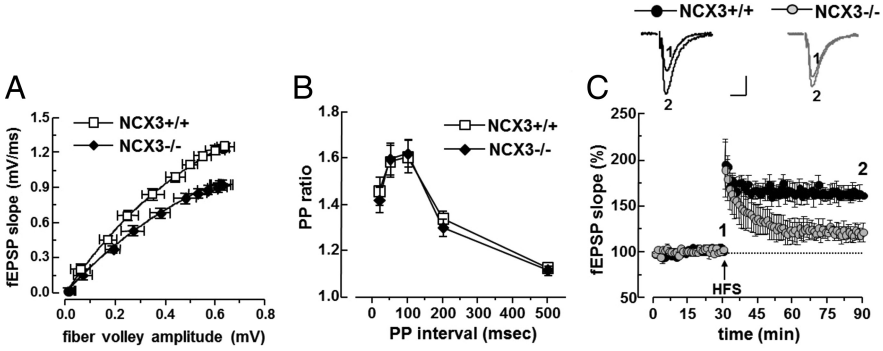

Figure 3. Synaptic function in *ncx3* $^{-/-}$ hippocampal slices. ***A***, Input/output curves for *ncx3* $^{-/-}$ and congenic wild-type mice measured by plotting the fEPSP slopes and their corresponding presynaptic fiber volley amplitudes at increasing stimulus strengths. Basal synaptic transmission was impaired in NCX3 knock-out mice compared with wild-type littermates ($n = 9$ slices from 7 animals, Student's *t* test, $p < 0.01$). Each data point is the mean of two recordings. ***B***, Paired-pulse (PP) facilitation between the two experimental groups ($p > 0.1$ for all comparisons). The facilitation ratio (slope of second EPSP/slope of first EPSP) was plotted as a function of interpulse intervals of 20, 50, 100, 200, and 500 ms. For each group, the mean ± SEM is indicated. ***C***, Superimposed pooled data showing the normalized changes in field potential slope (±SEM) induced by HFS in *ncx3* $^{-/-}$ ($n = 8$) and congenic *ncx3* $^{+/+}$ mice ($n = 6$). fEPSP slopes were recorded and were expressed as the percentage of the pretetanus baseline. Representative fEPSPs traces before and 60 min after the induction of LTP are shown. Calibration bars, 0.5 mV, 10 ms.

NCX3 disruption impairs basal-synaptic transmission and LTP in the hippocampus

To establish basal synaptic function in *ncx3* $^{-/-}$ mice, we generated input/output (I/O) curves by measuring fEPSPs elicited in the CA1 region by stimulation of the Schaffer collaterals at increasing stimulus intensities. As shown in Figure 3*A*, 2-month-old *ncx3* $^{-/-}$ mice had significantly reduced maximum fEPSPs compared with *ncx3* $^{+/+}$ mice, particularly when the presynaptic afferents were stimulated at higher intensities. Accordingly, the slopes of the input/output plots were reduced from $1.25 \pm 0.04\ V \cdot s^{-1} \cdot mV^{-1}$ ($n = 15$ slices from 10 animals) in the *ncx3* $^{+/+}$ to $0.92 \pm 0.05\ V \cdot s^{-1} \cdot mV^{-1}$ in the *ncx3* $^{-/-}$ mice ($n = 9$ slices from 7 animals, Student's *t* test, $p < 0.01$; Fig. 3*A*). These results imply that the decline in fast glutamatergic transmission was exacerbated in the absence of the NCX3 isoform. We then investigated PPF, a measure of short-term plasticity. The mechanisms underlying PPF are thought to be presynaptic (Zucker and Regehr, 2002) and probably involve residual Ca^{2+} in the nerve terminal after the first stimulus, a phenomenon that enhances neurotransmitter release during the second stimulus. No differences in the paired-pulse ratio between the two groups were observed ($p > 0.5$ at all interpulse intervals; Fig. 3*B*). Interestingly, we observed a significant decrease in the magnitude of LTP in *ncx3* $^{-/-}$ animals, compared with congenic control mice. Synaptic potentiation, measured 60 min after application of HFS, was 61 ± 4% above baseline ($n = 6$) in control but only 21 ± 10% ($n = 8$) in mutant slices ($p < 0.05$; Fig. 3*C*).

CaMKIIα expression is reduced in the CA1 region of the hippocampus where NCX3 colocalized with the postsynaptic marker PSD-95

The immunofluorescence analysis of the overall morphology of the hippocampal regions, performed with the neuronal marker NeuN in the CA1, CA2 and dentate gyrus subfields, did not show any significant morphological abnormalities of the hippocampus in either *ncx3* $^{-/-}$ or *ncx3* $^{+/+}$ experimental mice (Fig. 4*A*). In fact, immunofluorescence quantification of hippocampal NeuN expression revealed no significant differences between the two experimental groups (Fig. 4*B*).

Moreover, the quantification of synapse number in CA1 region, using synaptophysin as marker, revealed no differences between *ncx3* $^{+/+}$ and *ncx3* $^{-/-}$ mice (Fig. 4*C*,*D*). Accordingly, the total fluorescence intensity of synaptophysin in CA1 region of *ncx3* $^{-/-}$ mice was not significantly different from that of *ncx3* $^{+/+}$ mice (Fig. 4*E*).

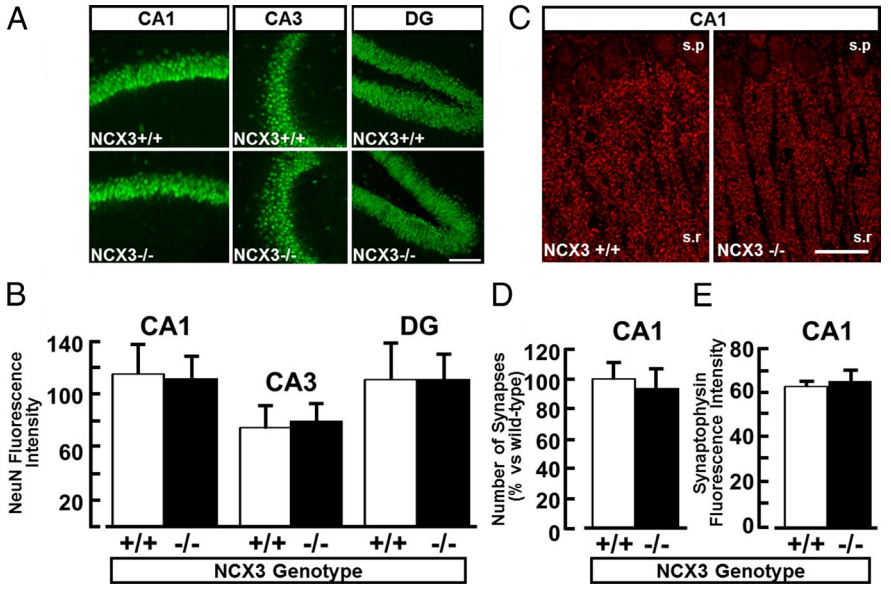

Figure 4. Morphological analysis of the hippocampus in *ncx3* $^{+/+}$ and *ncx3* $^{-/-}$ mice. ***A***, Immunofluorescence images of CA1, CA3, and DG in the hippocampus of NCX3 knock-out (bottom) and wild-type (top) mice. Comparison of NeuN-positive neurons did not show gross differences between the two experimental groups. Scale bar, 50 μm. ***B***, Quantification of NeuN fluorescence intensity in wild-type and knock-out mice. No significant differences were found between these two groups. ***C***, Immunofluorescence images showing synaptophysin puncta in CA1 region of NCX3 wild-type (left) and knock-out (right) mice. Scale bar, 20 μm. ***D***, Quantification of synaptophysin puncta number, expressed as percentage of wild-type, in CA1 regions of *ncx3* $^{+/+}$ ($n = 4$) and *ncx3* $^{-/-}$ ($n = 5$) mice. ***E***, Quantification of the fluorescence intensity, expressed as arbitrary units, in CA1 regions of *ncx3* $^{+/+}$ ($n = 4$) and *ncx3* $^{-/-}$ ($n = 5$) mice. s.p., Stratum pyramidalis; s.r., stratum radiatum. All data represent mean ± SEM.

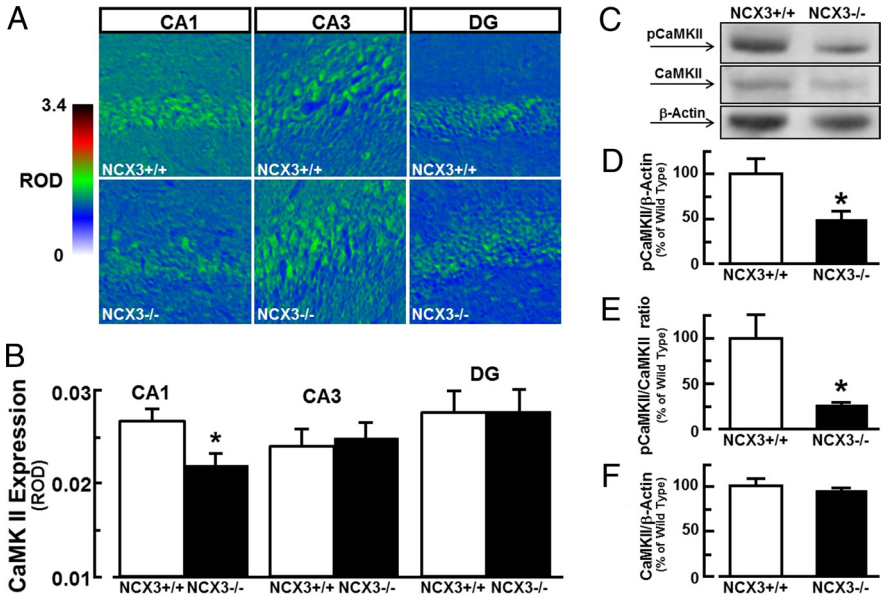

Figure 5. Quantification of CaMKIIα expression and phosphorylation in the hippocampus of *ncx3* $^{+/+}$ and *ncx3* $^{-/-}$ mice. ***A***, Representative images of hippocampal subfields stained with CaMKIIα antibody in *ncx3* $^{+/+}$ and *ncx3* $^{-/-}$ mice. ***B***, Quantification of CaMKIIα signal expressed as arbitrary optic density units. Each bar represents the mean (±SEM) of the immunofluorescence values obtained from hippocampal slices of 5 *ncx3* $^{+/+}$ mice and 7 *ncx3* $^{-/-}$ mice. *$p < 0.05$ versus congenic *ncx3* $^{+/+}$. ***C***, Western blot of phosphoCaMKIIα (pCaMKIIα), CaMKIIα, and β-actin in the whole hippocampus of *ncx3* $^{-/-}$ and *ncx3* $^{+/+}$ mice. ***D***, Quantification of the expression of phosphoCaMKIIα versus total CaMKIIα. ***E***, Quantification of the expression of phosphoCaMKIIα versus β-actin. *$p < 0.05$ versus congenic *ncx3* $^{+/+}$. ***F***, Quantificaiton of the expression of total CaMKIIa versus β-actin.

On the other hand, staining of *ncx3* $^{-/-}$ hippocampus slices did reveal that CaMKIIα expression, the main protein of the postsynaptic density at excitatory synapses, was significantly reduced by 27% in the CA1 region compared with the CA1 of congenic *ncx3* $^{+/+}$ (*ncx3* $^{+/+}$ $n = 5$; *ncx3* $^{-/-}$ $n = 7$; $p < 0.05$). However, no changes in CaMKIIα expression were detected in the CA3 and DG regions (Fig. 5*A*,*B*). Furthermore, phosphorylated form of CaMKIIα was reduced in hippocampus from *ncx3* $^{-/-}$ mice compared with *ncx3* $^{+/+}$ (49 ± 10% in *ncx3* $^{-/-}$ vs 100 ± 17% in *ncx3* $^{+/+}$; $p < 0.05$) (Fig. 5*C*,*D*). In addition, the ratio between the phosphorylated form of CaMKIIα and total CaMKIIα was significantly reduced in *ncx3* $^{-/-}$ compared with *ncx3* $^{+/+}$ mice (27 ± 3% in *ncx3* $^{-/-}$ vs 100 ± 21% in *ncx3* $^{+/+}$; $p < 0.05$) (Fig. 5*C*,*E*).

Confocal double immunofluorescence experiments performed in CA1 region with both NCX3 antibodies and the postsynaptic marker PSD-95 revealed that the percentage of colocalization between NCX3 and PSD-95-positive signals, expressed as the ratio between NCX3+ PDS95/NCX3 and NCX3− PDS95/NCX3 pixels, was 20.4 ± 4.6% (Fig. 6).

ncx3 $^{-/-}$ mice display a decreased performance in novel object recognition, fear conditioning, and spatial learning and memory

Open-field exploration

ncx3 $^{-/-}$ mice 6–8 weeks old did not differ significantly from congenic *ncx3* $^{+/+}$ animals in overall health and appearance, body weight, and core body temperature. Moreover, no apparent alterations in the spontaneous behavior of *ncx3* $^{-/-}$ mice were evident in the home cage.

To examine spontaneous locomotor activity and response to a novel environment, *ncx3* $^{+/+}$ and *ncx3* $^{-/-}$ mice were assayed in an open field test. These studies showed that NCX3 mutant mice did not differ from control animals in their locomotor and exploratory behavior (distance traveled in 5 min: *ncx3* $^{+/+}$, 2592 ± 251 cm, $n = 9$; *ncx3* $^{-/-}$, 2467 ± 136 cm, $n = 14$) (Fig. 7*A*).

To study whether the lack of NCX3 affected anxiety related behavior, the time spent by animals in the center of the arena was compared with that spent in the region close to the walls. As this time is related to the size of the central region considered, we evaluated the exploration time in three concentric rectangular regions having a perimeter equivalent to 3/4, 1/2, and 1/4 of the original arena (Fig. 7*C*). The time spent by *ncx3* $^{-/-}$ mice in the three concentric regions did not differ significantly from the time spent by the congenic *ncx3* $^{+/+}$ animals (Fig. 7*B*). Moreover, the defecation score was not significantly different between the two groups

($ncx3^{+/+}$, 2 boluses, $n = 9$; $ncx3^{-/-}$, 0.92, $n = 14$; $p > 0.05$ Kruskal–Wallis test), thus suggesting that the lack of NCX3 does not alter anxious behavior.

One-trial object recognition task

The amount of time spent with the novel object compared with the total time spent exploring both objects represents an index of long-term memory. During training, animals showed no preference for one object over another and there was no difference between $ncx3^{+/+}$ and $ncx3^{-/-}$ mice in the exploration time, suggesting that the experimental groups were on average equally motivated to explore objects (Fig. 8*A*). However, when presented with a novel object, $ncx3^{+/+}$ animals showed a preference for the new one after 2 or 24 h of retention ($n = 8$ and 7, respectively). In contrast, $ncx3^{-/-}$ mice showed a significant lower preference for novel objects when compared $ncx3^{+/+}$ mice (Fig. 8*B*).

Trace Fear Conditioning

When exposed to the context, $ncx3^{-/-}$ mice showed a reduced freezing response compared with $ncx3^{+/+}$ mice ($ncx3^{-/-}$, 18.9 ± 6.2%, $n = 8$; $ncx3^{+/+}$, 45.8 ± 11.2%, $n = 6$; $p < 0.05$ one-tailed Student's t test for nonpaired data). Similar results were obtained when exposed to tone test, $ncx3^{-/-}$ mice showed a reduced freezing response compared with $ncx3^{+/+}$ mice ($ncx3^{-/-}$, 8.8 ± 2.2%, $n = 8$; $ncx3^{+/+}$, 25.3 ± 6.7%, $n = 6$, $p < 0.05$ one-tailed Student's t test for nonpaired data). The trace fear conditioning assay is a Pavlovian form of learning which requires the integrity of the hippocampus. In tone test, $ncx3^{+/+}$ ($n = 7$) and $ncx3^{-/-}$ ($n = 6$) mice showed different durations of freezing response when exposed to the tone stimulus in a new chamber 2 h after the conditioning. Results showed that $ncx3^{-/-}$ mice have an impaired fear memory compared with congenic $ncx3^{+/+}$ mice (Fig. 8*E*).

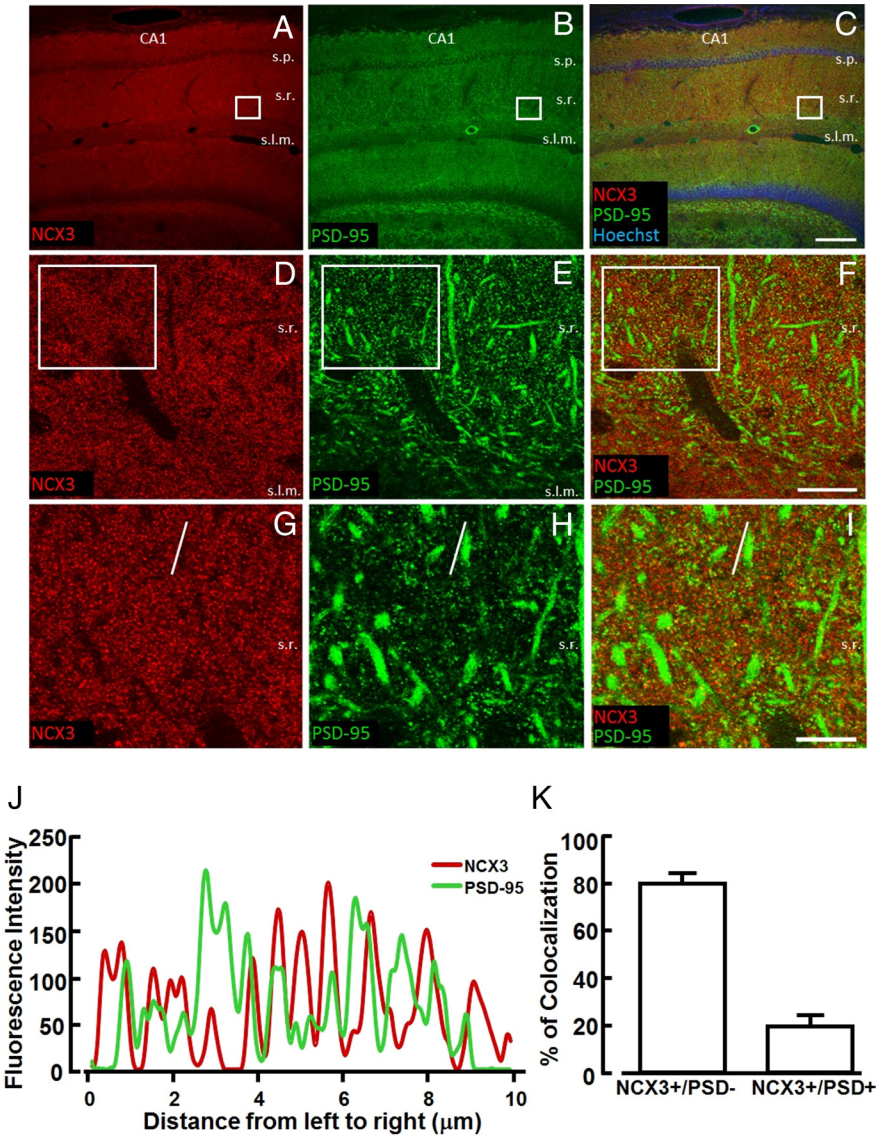

Figure 6. Colocalization of NCX3 with PSD-95 in the CA1 hippocampal region. ***A–C***, Confocal microscopic images depicting NCX3 (red) and PSD-95 (green) immunoreactivity in the CA1 region of adult mouse hippocampus. In C, nuclei in pyramidal and granule cell layers are stained with Hoechst-33258 (blue). ***D–F***, Higher-magnification images of the boxes depicted in ***A–C***, showing partial overlapping of NCX3 and PSD-95 labeling in the stratum radiatum. ***G–I***, Higher magnification of boxes depicted in D–F displaying colocalization of some PSD-95-positive puncta with NCX3 punctuate labeling. ***J***, Spatial profile plot of pixel intensity of NCX3 (red) and PSD-95 (green) along the line indicated in panels G and H, demonstrating the spatial overlap of individual puncta positive for NCX3 and PSD-95. ***K***, Quantification of the percentage of colocalization between NCX3- and PSD-95-positive signals in ***I***, expressed as the ratio between NCX3+ PDS-95/NCX3 and NCX3− PDS-95/NCX3 pixels. s.o., Stratum oriens, s.p., stratum pyramidale; s.r, stratum radiatum; s.l.m., stratum lacunosum moleculare. Scale bars: ***A–C***, 200 μm; ***D–F***, 20 μm; ***G–I***, 10 μm.

Barnes circular maze task

The learning and memory performance of $ncx3^{+/+}$ and $ncx3^{-/-}$ mice was also evaluated by means of the Barnes circular maze test, a hippocampus-dependent cognitive task that requires spatial reference memory (Barnes, 1979, 1988; Bach et al., 1995). Congenic $ncx3^{+/+}$ mice after the third day showed a significant reduction in the escape latency which progressively decreased until the sixth day (Fig. 8*D*). In contrast, $ncx3^{-/-}$ ($n = 21$) mice did not show any significant changes in escape latencies after the third day and until the sixth day. These escape latencies values were significantly higher at days 4–6 in $ncx3^{-/-}$ mice than those observed in congenic $ncx3^{+/+}$ (Fig. 8*D*). These results showed that mice lacking ncx3 alleles did not learn to locate the escape hole during the period of observation (days 1–6), thus suggesting an impairment of the spatial learning and memory performance.

Discussion

The results of the present study demonstrate that NCX3 gene ablation, by delaying $[Ca^{2+}]_i$ clearance after neuronal activation, decreases the magnitude of LTP at hippocampal Schaffer collateral-CA1 synapse level, without affecting short-term plasticity. In accordance with these electrophysiological data, NCX3 knock-out mice showed a significant reduction in hippocampus-dependent spatial-learning and memory performance.

The impairment of LTP in the CA1 subregion could be due to a dysregulation of $[Ca^{2+}]_i$ homeostasis elicited by the reduction of NCX currents in the forward mode of operation after the ge-

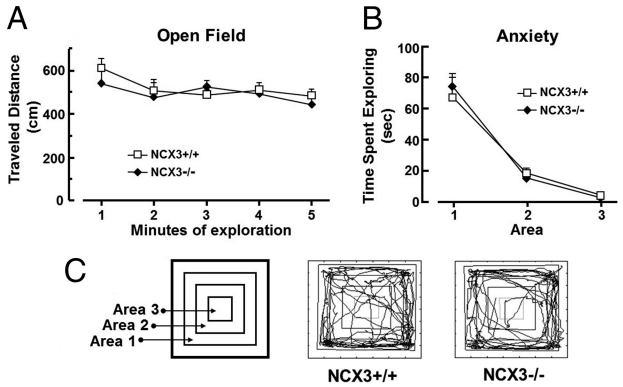

Figure 7. Locomotor activity and anxiety levels in *ncx3* $^{+/+}$ and *ncx3* $^{-/-}$ mice. ***A***, Locomotor activity of NCX3 knock-out versus congenic wild-type mice in the open field test. Total traveled distance was measured using an automated tracking device. The distance traveled in 5 min was the following: *ncx3* $^{+/+}$, 2592 ± 251 cm, $n = 9$; *ncx3* $^{-/-}$, 2467 ± 136 cm, $n = 14$. ***B***, Quantification of the time spent by animals in three concentric areas measured as anxious behavior test of NCX3 knock-out mice versus congenic wild-type mice. (*ncx3* $^{+/+}$, $n = 9$; *ncx3* $^{-/-}$, $n = 14$). ***C***, Representative subdivision of the cage apparatus used in the open field test (left) and two representative drawings of the automated tracking system of congenic wild-type (center) and NCX3 knock-out (right) mice.

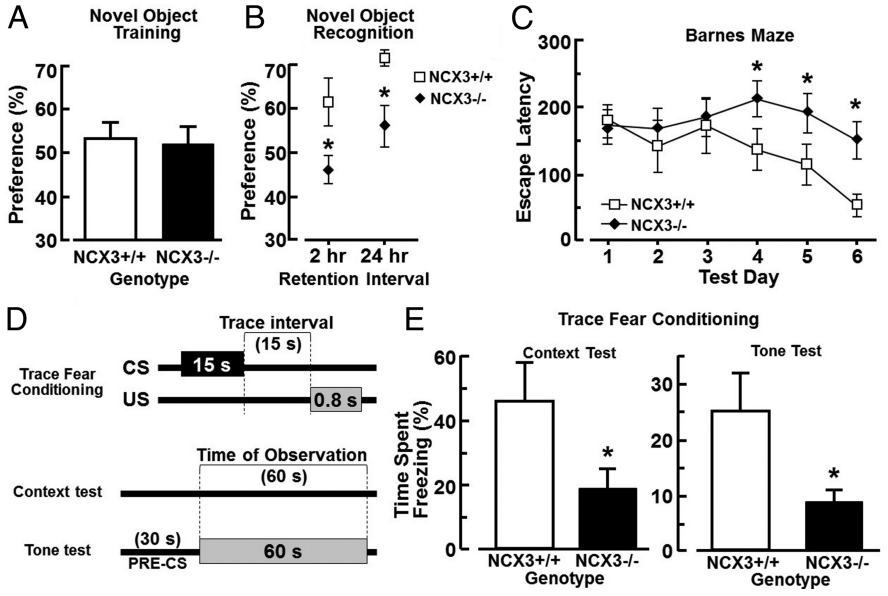

Figure 8. Hippocampal-dependent long-term memory test measured in NCX3 $^{+/+}$ and NCX $^{-/-}$ mice. ***A***, Percentage of preference between two objects in the training phase of the novel object test performed in NCX3 knock-out and congenic wild-type mice. ***B***, Percentage of preference in the trial phase of the novel object recognition test 2 and 24 h after the training phase (2 h, $n = 8$ for each group; 24 h, $n = 7$ for each group). *$p < 0.05$ versus wild-type mice. Dashed line indicates equal exploration time spent for all objects. ***C***, Results of NCX3 $^{-/-}$ and congenic NCX3 $^{+/+}$ mice subjected to Barnes maze test during 6 d of training as revealed by two-way ANOVA with repeated measures across training days, and as assessed by one-way Dunnett's test for repeated comparisons ($n = 21$ for each group). *$p < 0.05$. ***D***, Schematic representation of the temporal relationship between the CS and US for a single trial. The trace interval ensures that the task is sensitive to hippocampal function (Bangasser et al., 2006). ***E***, Percentage of total time spent in the freeze status when NCX3 $^{-/-}$ and congenic NCX3 $^{+/+}$ mice were exposed to context or tone test.

reduction in basal synaptic transmission, and a reduction in LTD (Wu et al., 2010). Conversely, knock-out mice of the NCX3 transcriptional repressor DREAM display enhanced learning and memory performance (Fontán-Lozano et al., 2009).

Interestingly, CaMKIIα expression was significantly reduced in the CA1 area of *ncx3* $^{-/-}$ mice. This alteration does not seem to be ascribed to changes in the number of neurons or of synapses, since NeuN-positive neurons and synaptophysin-positive puncta were not changed in *ncx3* $^{-/-}$ mice. Moreover, the ratio between the phosphorylated form of CaMKIIα and the total CaMKIIα was significantly reduced. This reduction in knock-out mice may also explain LTP impairment at hippocampal Schaffer collateral-CA1 synapses. In fact, pharmacological data and transgenic mice studies support the idea that CaMKIIα has a crucial role in the CA1 area for LTP at postsynaptic level. Indeed, the use of specific pharmacological inhibitors of the enzyme in the CA1 area or the genetic deletion of CaMKIIα impairs LTP and, consequently, hippocampus-dependent spatial-learning and memory (Silva et al., 1992a,b). Moreover, LTP was reduced in *ncx3* $^{-/-}$ mice, as demonstrated by the reduction of the fEPSP slope from the CA1 area of the hippocampus in response to stimulation of Schaffer collateral fibers. In addition, *ncx3* $^{-/-}$ hippocampal slices showed a reduced basal synaptic transmission as demonstrated by the reduced maximum fEPSP slope. The reduction of this latter phenomenon cannot be related, at the present time, with the reduction of CaMKIIα activity and LTP, as it might also depend on other mechanisms such as the organization and number of dendritic spines, the activity of excitatory amino acid receptor and ryanodine receptor.

Altogether these results, along with the experimental data on paired pulse facilitation, which excluded possible alterations in neurotransmitter release, suggest that NCX3KO-induced LTP derangement occurred predominantly at postsynaptic level. In fact, morphological data obtained in the present paper show that at least 20% of the whole NCX3 staining colocalized in the CA1 subfield with PSD-95, a postsynaptic marker.

Another aspect that should be analyzed is the relationship among the elevated basal level of $[Ca^{2+}]_i$ in hippocampal neurons, the reduction of the expression and the activity of CaMKIIα in the hippocampus, and the consequent impairment of LTP observed in *ncx3* $^{-/-}$ mice. Interestingly, Lisman (2001) proposed that different levels of $[Ca^{2+}]_i$ may produce opposite effects on CaMKIIα activation. In particular, a moderate elevation of $[Ca^{2+}]_i$ activates a phosphatase cascade with a dephosphorylation of CaMKIIα and with a reduction of its activity (Lisman, 2001). By contrast, when higher $[Ca^{2+}]_i$ elevation occurs, as during LTP induction, the phosphatase cascade is inhibited and CaMKIIα is phosphorylated thus increasing its activity. It is likely that the knock-out of NCX3 in hippocampal neurons provokes a moderate elevation of $[Ca^{2+}]_i$ in resting conditions that, in turn, might activate the phosphatase cascade with a consequent decrease in the phosphorylated form of

netic ablation of ncx3 gene. This hypothesis is supported by the increased level of $[Ca^{2+}]_i$ observed in resting conditions and the impaired clearance of $[Ca^{2+}]_i$ following neuronal depolarization in *ncx3* $^{-/-}$ hippocampal neurons. Consistent with our findings is that in the hippocampus, the inhibition of NCX3 transcription, obtained in transgenic mice by overexpressing a constitutive active mutant of the NCX3 repressor, named DREAM (downstream regulatory element antagonist modulator), induces an increased level of $[Ca^{2+}]_i$ (Gomez-Villafuertes et al., 2005), a

CaMKIIα versus the total CaMKIIα, as Western blot analysis revealed. Therefore, *ncx3*$^{-/-}$ hippocampal neurons could have a decreased levels of the activated form of CaMKIIα with a consequent impairment of LTP and a decreased performance in spatial learning and memory. Indeed, the observations emerging from the three different hippocampus-dependent tasks used in this study, such as novel object recognition, Barnes maze, and fear conditioning tests, demonstrated that NCX3 genetic disruption impairs LTP without interfering with anxiety levels.

At variance with the results of the present study, Jeon et al. (2003) recently demonstrated that mice lacking the other isoform of the exchanger, NCX2, display an enhancement of synaptic plasticity at the presynaptic level, since both PPF and post-tetanic potentiation are enhanced. Furthermore, the reinforcement of LTP in mice lacking NCX2 is accompanied by an improvement in learning and memory performance.

Although the opposite roles played by NCX2 and NCX3 in LTP modulation, learning and memory processes cannot be explained on the basis of the present knowledge, several evidences might help to explain such differences. First, NCX2 is the only isoform of the exchanger that is present in the membrane of synaptic vesicles (Takamori et al., 2006). Second, unlike *ncx2*$^{-/-}$ neurons, hippocampal neurons of mice lacking NCX3 have higher levels of $[Ca^{2+}]_i$ than *ncx3*$^{+/+}$ in resting conditions. Third, *ncx3*$^{-/-}$ mice show a decreased basal synaptic transmission, whereas this phenomenon does not occur in *ncx2*$^{-/-}$ mice. Finally, in mice lacking NCX3 the impairment of LTP seems to occur mainly at the postsynaptic level, whereas in *ncx2*$^{-/-}$ mice, LTP is mostly modulated at the presynaptic level.

Therefore, further studies on the subcellular localization and function of the three isoforms of NCX are required to clarify the differential roles of NCX2 and NCX3 in the regulation of LTP.

The significant role of NCX3 in the hippocampal spatial learning and memory processes, emerged from the present study, may open new experimental avenues for the development of effective therapeutic compounds that, by selectively activating this molecular target, could treat patients affected by cognitive impairment including Alzheimer's, Parkinson's, Huntington's diseases and infarct dementia. Until now, no activators of NCX3 isoform are available. However since several inhibitors have been synthesized in the last few years, these compounds could be used as scaffold molecules for the development of selective NCX3 activators able to improve learning and memory deficits.

References

Annunziato L, Pignataro G, Di Renzo GF (2004) Pharmacology of brain Na+/Ca^{2+} exchanger: from molecular biology to therapeutic perspectives. Pharmacol Rev 56:633–654.

Bach ME, Hawkins RD, Osman M, Kandel ER, Mayford M (1995) Impairment of spatial but not contextual memory in CaMKII mutant mice with a selective loss of hippocampal LTP in the range of the theta frequency. Cell 81:905–915.

Bangasser DA, Waxler DE, Santollo J, Shors TJ (2006) Trace conditioning and the hippocampus: the importance of contiguity. J Neurosci 26:8702–8706.

Barnes CA (1979) Memory deficits associated with senescence: a neurophysiological and behavioral study in the rat. J Comp Physiol Psychol 93:74–104.

Barnes CA (1988) Spatial learning and memory processes: the search for their neurobiological mechanisms in the rat. Trends Neurosci 11:163–169.

Boscia F, Gala R, Pignataro G, de Bartolomeis A, Cicale M, Ambesi-Impiombato A, Di Renzo G, Annunziato L (2006) Permanent focal brain ischemia induces isoform-dependent changes in the pattern of Na+/Ca^{2+} exchanger gene expression in the ischemic core, periinfarct area, and intact brain regions. J Cereb Blood Flow Metab 26:502–517.

Burke RE, Cadet JL, Kent JD, Karanas AL, Jackson-Lewis V (1990) An assessment of the validity of densitometric measures of striatal tyrosine hydroxylase-positive fibers: relationship to apomorphine-induced rotations in 6-hydroxydopamine lesioned rats. J Neurosci Methods 35:63–73.

Capowski JJ (1989) Computer techniques in neuroanatomy. New York: Plenum.

Carlucci A, Adornetto A, Scorziello A, Viggiano D, Foca M, Cuomo O, Annunziato L, Gottesman M, Feliciello A (2008) Proteolysis of AKAP121 regulates mitochondrial activity during cellular hypoxia and brain ischaemia. EMBO J 27:1073–1084.

D'Adamo P, Welzl H, Papadimitriou S, Raffaele di Barletta M, Tiveron C, Tatangelo L, Pozzi L, Chapman PF, Knevett SG, Ramsay MF, Valtorta F, Leoni C, Menegon A, Wolfer DP, Lipp HP, Toniolo D (2002) Deletion of the mental retardation gene Gdi1 impairs associative memory and alters social behavior in mice. Hum Mol Genet 11:2567–2580.

Dere E, Huston JP, De Souza Silva MA (2007) The pharmacology, neuroanatomy and neurogenetics of one-trial object recognition in rodents. Neurosci Biobehav Rev 31:673–704.

Desmedt A, Marighetto A, Garcia R, Jaffard R (2003) The effects of ibotenic hippocampal lesions on discriminative fear conditioning to context in mice: impairment or facilitation depending on the associative value of a phasic explicit cue. Eur J Neurosci 17:1953–1963.

Ennaceur A, Delacour J (1988) A new one-trial test for neurobiological studies of memory in rats. 1: Behavioral data. Behav Brain Res 31:47–59.

Fontán-Lozano A, Romero-Granados R, del-Pozo-Martín Y, Suárez-Pereira I, Delgado-García JM, Penninger JM, Carrión AM (2009) Lack of DREAM protein enhances learning and memory and slows brain aging. Curr Biol 19:54–60.

Gomez-Villafuertes R, Torres B, Barrio J, Savignac M, Gabellini N, Rizzato F, Pintado B, Gutierrez-Adan A, Mellström B, Carafoli E, Naranjo JR (2005) Downstream regulatory element antagonist modulator regulates Ca^{2+} homeostasis and viability in cerebellar neurons. J Neurosci 25:10822–10830.

Grynkiewicz G, Poenie M, Tsien RY (1985) A new generation of Ca^{2+} indicators with greatly improved fluorescence properties. J Biol Chem 260:3440–3450.

Huerta PT, Sun LD, Wilson MA, Tonegawa S (2000) Formation of temporal memory requires NMDA receptors within CA1 pyramidal neurons. Neuron 25:473–480.

Jeon D, Yang YM, Jeong MJ, Philipson KD, Rhim H, Shin HS (2003) Enhanced learning and memory in mice lacking Na+/Ca^{2+} exchanger 2. Neuron 38:965–976.

Kassed CA, Herkenham M (2004) NF-kappaB p50-deficient mice show reduced anxiety-like behaviors in tests of exploratory drive and anxiety. Behav Brain Res 154:577–584.

Kazlauckas V, Schuh J, Dall'Igna OP, Pereira GS, Bonan CD, Lara DR (2005) Behavioral and cognitive profile of mice with high and low exploratory phenotypes. Behav Brain Res 162:272–278.

Lisman JE (2001) Three Ca^{2+} levels affect plasticity differently: the LTP zone, the LTD zone and no man's land. J Physiol 532:285.

Lu YM, Jia Z, Janus C, Henderson JT, Gerlai R, Wojtowicz JM, Roder JC (1997) Mice lacking metabotropic glutamate receptor 5 show impaired learning and reduced CA1 long-term potentiation (LTP) but normal CA3 LTP. J Neurosci 17:5196–5205.

McEchron MD, Bouwmeester H, Tseng W, Weiss C, Disterhoft JF (1998) Hippocampectomy disrupts auditory trace fear conditioning and contextual fear conditioning in the rat. Hippocampus 8:638–646.

Molinaro P, Cuomo O, Pignataro G, Boscia F, Sirabella R, Pannaccione A, Secondo A, Scorziello A, Adornetto A, Gala R, Viggiano D, Sokolow S, Herchuelz A, Schurmans S, Di Renzo G, Annunziato L (2008) Targeted disruption of Na+/Ca^{2+} exchanger 3 (NCX3) gene leads to a worsening of ischemic brain damage. J Neurosci 28:1179–1184.

Papa M, Canitano A, Boscia F, Castaldo P, Sellitti S, Porzig H, Taglialatela M, Annunziato L (2003) Differential expression of the Na+-Ca^{2+} exchanger transcripts and proteins in rat brain regions. J Comp Neurol 461:31–48.

Pignataro G, Gala R, Cuomo O, Tortiglione A, Giaccio L, Castaldo P, Sirabella R, Matrone C, Canitano A, Amoroso S, Di Renzo G, Annunziato L (2004) Two sodium/calcium exchanger gene products, NCX1 and NCX3, play a major role in the development of permanent focal cerebral ischemia. Stroke 35:2566–2570.

Quednau BD, Nicoll DA, Philipson KD (1997) Tissue specificity and alter-

native splicing of the $Na+/Ca^{2+}$ exchanger isoforms NCX1, NCX2, and NCX3 in rat. Am J Physiol 272:C1250–C1261.

Reuter H, Porzig H (1995) Localization and functional significance of the $Na+/Ca^{2+}$ exchanger in presynaptic boutons of hippocampal cells in culture. Neuron 15:1077–1084.

Secondo A, Staiano RI, Scorziello A, Sirabella R, Boscia F, Adornetto A, Valsecchi V, Molinaro P, Canzoniero LM, Di Renzo G, Annunziato L (2007) BHK cells transfected with NCX3 are more resistant to hypoxia followed by reoxygenation than those transfected with NCX1 and NCX2: possible relationship with mitochondrial membrane potential. Cell Calcium 42:521–535.

Seeger T, Fedorova I, Zheng F, Miyakawa T, Koustova E, Gomeza J, Basile AS, Alzheimer C, Wess J (2004) M2 muscarinic acetylcholine receptor knock-out mice show deficits in behavioral flexibility, working memory, and hippocampal plasticity. J Neurosci 24:10117–10127.

Silva AJ, Stevens CF, Tonegawa S, Wang Y (1992a) Deficient hippocampal long-term potentiation in alpha-calcium-calmodulin kinase II mutant mice. Science 257:201–206.

Silva AJ, Paylor R, Wehner JM, Tonegawa S (1992b) Impaired spatial learning in alpha-calcium-calmodulin kinase II mutant mice. Science 257:206–211.

Skeberdis VA, Chevaleyre V, Lau CG, Goldberg JH, Pettit DL, Suadicani SO, Lin Y, Bennett MV, Yuste R, Castillo PE, Zukin RS (2006) Protein kinase A regulates calcium permeability of NMDA receptors. Nat Neurosci 9:501–510.

Sokolow S, Manto M, Gailly P, Molgó J, Vandebrouck C, Vanderwinden JM, Herchuelz A, Schurmans S (2004) Impaired neuromuscular transmission and skeletal muscle fiber necrosis in mice lacking Na/Ca exchanger 3. J Clin Invest 113:265–273.

Takamori S, Holt M, Stenius K, Lemke EA, Grønborg M, Riedel D, Urlaub H, Schenck S, Brügger B, Ringler P, Müller SA, Rammner B, Gräter F, Hub JS, De Groot BL, Mieskes G, Moriyama Y, Klingauf J, Grubmüller H, Heuser J, et al. (2006) Molecular anatomy of a trafficking organelle. Cell 127:831–846.

Wu LJ, Mellström B, Wang H, Ren M, Domingo S, Kim SS, Li XY, Chen T, Naranjo JR, Zhuo M (2010) DREAM (downstream regulatory element antagonist modulator) contributes to synaptic depression and contextual fear memory. Mol Brain 3:3.

Zucker RS, Regehr WG (2002) Short-term synaptic plasticity. Annu Rev Physiol 64:355–405.